Published in final edited form as:

Nature. 2013 May 23; 497(7450): 482–485. doi:10.1038/nature12077.

Corticostriatal neurones in auditory cortex drive decisions during auditory discrimination

Petr Znamenskiy[1,2] and **Anthony M. Zador**[2]

[1]Watson School of Biological Sciences, Cold Spring Harbor Laboratory, Cold Spring Harbor, NY, USA

[2]Cold Spring Harbor Laboratory, Cold Spring Harbor, NY, USA

Abstract

The neural pathways by which information about the acoustic world reaches the auditory cortex are well characterised, but how auditory representations are transformed into motor commands is not known. Here we have used a perceptual decision-making task to study this transformation. We directly demonstrate the role of corticostriatal projection neurones in auditory decisions by specifically manipulating the activity of these neurones in rats performing an auditory frequency discrimination task. Targeted Channelrhodopsin-2[1,2] (ChR2)-mediated stimulation of corticostriatal neurones during the task biased decisions in the direction predicted by the frequency tuning of the stimulated neurones, whereas archaerhodopsin-3[3] (Arch)-mediated inactivation biased decisions in the opposite direction. Striatal projections are widespread in cortex and may provide a general mechanism for the control of motor decisions by sensory cortex.

Upon reaching the cortex, auditory information is processed and relayed to a number of cortical and subcortical targets by distinct, largely non-overlapping populations of pyramidal neurones. These targets include parietal cortex, secondary auditory areas, inferior colliculus and striatum, regions which play distinct roles in perception and behaviour. How these outputs help establish associations between sounds and motor responses is unknown.

We hypothesized that the projection from the auditory cortex to the striatum carries acoustic information that drives behavioural choices during auditory discrimination. The striatum receives topographic inputs from throughout the cortex. Striatal regions which receive input from motor and prefrontal cortices have been implicated in a wide range of cognitive processes, including decision-making[4], action selection[5], and reinforcement learning[6,7]. Through downstream structures of the basal ganglia, the striatum influences the activity in

*Corresponding: zador@cshl.edu.

Supplementary Information is linked to the online version of the paper at www.nature.com/nature.

Author Contributions

P.Z. and A.M.Z. designed the experiments; P.Z. performed the experiments; P.Z. and A.M.Z. analyzed the data and wrote the manuscript.

The authors declare no competing financial interests.

the motor thalamus[8] as well as superior colliculus[9], a structure which has been implicated in driving behavioural choices in 2-AFC tasks[10]. Plasticity of corticostriatal connections may enable them to encode the arbitrary stimulus-response associations acquired in such tasks[11].

By contrast, the function of striatal regions which receive direct input from sensory cortical areas is less well established. The striatum is one of the major long range targets of the auditory cortex[12]. The auditory cortex projects to a specific region of the striatum[13]. This striatal region does not receive input from any other cortical area and contains neurones sensitive to auditory stimuli[14,15]. We set out to test whether the auditory corticostriatal projection drives choices during auditory discrimination.

We first developed a novel auditory discrimination task, inspired by experiments in primate area MT[16], which was designed to exploit the tonotopic organization of the auditory system[17]. We trained rats to discriminate low and high frequency “cloud-of-tones” stimuli in a two alternative choice task[18] (Fig. 1a). On each trial the stimulus consisted of a train of short overlapping pure tones distributed over a three octave range (5–40 kHz). Subjects were required to choose between a left and a right reward port depending on whether the stimulus contained mostly low (5–10 kHz) or high (20–40 kHz) frequency tones (Fig. 1b). Rats were free to withdraw and report their choice at any time after the onset of the stimulus. Rats readily learned this task. Performance varied smoothly with stimulus difficulty, and approached 100% on the easiest stimuli (Fig. 1c).

We used tetrode recordings to characterize the activity of individual neurones in the auditory cortex and the auditory striatum while rats performed the task. Auditory striatal neurones have previously been characterized in anaesthetised and passively listening animals[14,15] not during behaviour. The firing rates of neurones in both auditory cortex and striatum varied monotonically with the stimulus (Fig. S1abef). “Ideal observer” analysis showed that stimulus selectivity of cortical and striatal neurons was similar (Fig. S1cdgh). Although individual neurones rarely matched the performance of the rats, many neurones in both areas could discriminate the stimulus above chance levels (Fig. S1dh). These observations indicate that neurones in the striatum preserve the information available to perform the ”cloud-of-tones” task.

We then tested whether manipulating cortical activity with ChR2[1,2] could affect subjects’ choices in the task. We hypothesized that activation of auditory cortical neurones in different regions of the tonotopic map would result in choice biases, the direction of which would depend on the frequency-response association the rat had been trained to make. We implanted arrays of optical fibers coupled to tetrodes (Fig. S2), which allowed us to characterize the frequency preference of neurones near the fiber tip. We activated ChR2-expressing auditory cortex neurones on a subset of trials, and compared performance on stimulated trials to that on control trials without light activation. To minimize behavioural adaptation to photostimulation we limited the number of stimulation trials to 25%, and rewarded the animal as on control trials according to the frequency content of the stimulus. To quantify the effects of photostimulation on subjects’ behaviour, we fit a logistic regression model to the subjects’ choices (see Methods), estimating what change to the auditory stimulus would produce a behavioural effect equivalent to that of photostimulation.

We first expressed ChR2 non-specifically in the primary auditory cortex using adeno-associated virus (AAV). ChR2 expression was distributed throughout layers II–V and to a lesser extent layer VI (Fig. S3ab). On some sessions activation of ChR2-expressing neurones induced substantial biases (Fig. S3c). Contrary to our expectations, however, the direction of the bias was not predicted by the tuning of the neurones near the fiber (Fig. S3f). Moreover, this non-specific activation not only biased subjects' choices, but also interfered with their ability to perform the task, as measured by the slope of the psychometric curve (Fig. S3de).

The lack of correspondence between the direction of stimulation-evoked choice biases and frequency tuning was surprising and has several possible explanations. First, these choice biases may result from activation of intracortical projection neurones from other frequency bands of the auditory cortex. Second, they may arise from preferential activation of local interneurones in response to synchronous activation of a large number of cortical cells. Third, these biases may be a consequence of stimulation of competing output pathways, projecting to target areas with different functional roles. Consistent with the latter possibility, stimulation resulted in predominantly contralateral biases (36/57 sites, $p = 0.015$, Fig. S3gh), suggesting the activation of a lateralized motor pathway. These results suggested that the auditory cortex plays a role in the task, but that the method of non-specific activation of diverse neuronal populations used in these experiments does not provide sufficient experimental control over the activity of the projection neurones driving choices in this behaviour. We therefore hypothesized that targeted stimulation of corticostriatal neurones might yield more systematic effects.

We used two complementary strategies to test the role of the neuronal subpopulation in auditory cortex that projects to the striatum. In the first strategy, we targeted ChR2 specifically to corticostriatal neurones using a Herpes Simplex Virus-1 (HSV1) engineered to express Cre recombinase[19,20,21] (Fig. 2a). This virus, when injected into the auditory striatum, was transported retrogradely along the axons and drove Cre expression in corticostriatal neurones. We then injected a Cre-dependent AAV driving expression of ChR2 into the auditory cortex, resulting in expression of ChR2 only in neurones infected by both the HSV1-Cre and the AAV-ChR2. Most (84%) of ChR2-expressing neurons were located in layer V (Fig. 2cd) consistent with previous results[22].

Pulses of blue light delivered through fibers in the cortex reliably drove action potentials a small population of presumed corticostriatal neurones (Fig. 2b, 4 of 201 cells responded on >50% of trials). Across sites, stimulation consistently biased subjects' choices toward the choice port associated with the preferred frequency of the stimulation site (Fig. 2ef). The biases were not significant on individual sessions ($p<0.05$ on 1/33 sessions), in part because the number of stimulated trials per session was typically small (70±24 (s.d.) trials). In contrast to non-specific stimulation, contralateral and ipsilateral biases were observed with similar frequency (12/33 contralateral sites, $p = 0.31$ signed-rank test) and subjects' psychophysical performance was not impaired (Fig. S4a). Choice biases were not observed in uninjected controls (Fig. 2g, S5a) indicating that they were driven by the ChR2-mediated activation of corticostriatal neurones and not non-specific effects of light delivery. Thus

activation of corticostriatal neurones biased behaviour in a manner predicted by their frequency tuning.

The behavioural effects of photostimulation could arise either directly through excitation of striatal neurones by their cortical inputs, or indirectly through excitation of other output pathways of the auditory cortex through recurrent connections. Excitation of corticostriatal neurones resulted in general suppression of local cortical activity (Fig. S6), favouring the hypothesis that behavioural effects of photostimulation are mediated by long-range rather than local outputs of these neurones.

To test this hypothesis directly, we used a second strategy which did not rely on cortical stimulation and thus would allow us to test whether stimulation of corticostriatal neurones could bias subjects' choices when recurrent cortical activity is blocked. We stimulated the axons of corticostriatal neurones in the striatum while inhibiting the recurrent cortical excitation pharmacologically (Fig. 2h). To define the frequency tuning of stimulated fibers, we exploited the topography of corticostriatal projections[23]. We confirmed the topographic organization of the striatal projection of the auditory cortex in rats through retrograde (Fig. S7) tracing. Owing to this topography, focal light stimulation in the striatum excites corticostriatal axons arising from a restricted region of the tonotopic map. We used striatal multiunit activity to characterize the frequency preference of the striatal stimulation site.

Stimulation of corticostriatal axons biased subjects' choices toward the choice port associated with the preferred frequency of the stimulation site (Fig. 2g, S5b). Stimulation also had a modest effect on the subjects' performance at sites with large choice biases, possibly due to a ceiling effect (Fig. S4bc). Thus both direct activation of corticostriatal somata in the cortex, as well as antidromic activation of corticostriatal terminals in the striatum, biased the rats' choices in a manner predicted from the frequency tuning of the activated neurones.

We next tested whether stimulation of the axons of corticostriatal neurones could bias subjects' choices in the absence of cortical recurrent activity. We selected striatal sites whose stimulation produced significant ($p < 0.05$) biases in subjects' choices and repeated stimulation after pharmacologically inactivating the ipsilateral auditory cortex. Cortical inactivation (2% lidocaine $n = 2$ sites, 125 μM tetrodotoxin $n = 5$ sites) blocked antidromic light-evoked local field potentials (Fig. 2i). Photostimulation of corticostriatal axons still biased choices in the absence of cortical activity ($p = 0.016$, signed-rank test, Fig. S8,S9), demonstrating that these biases are mediated directly by long-range outputs of corticostriatal neurones.

We next examined the effects of stimulation of corticostriatal neurons on rats' response times. Although individual rats varied in how they weighed response speed versus response accuracy (Fig. S10a–f), most rats used in the stimulation and inactivation experiments showed a small but significant (of order 20–50 ms) increase in response time on challenging trials, consistent with that reported previously in rats[18]. We quantified the shift of the chronometric curve produced by stimulation of corticostriatal neurons (Fig. S10gh). Across sessions stimulation shifted chronometric curves, mimicking the effect of adding acoustic

evidence favouring the choice associated with the preferred frequency of the stimulation site (Fig. S10ij).

Our results so far establish that activation of the corticostriatal pathway is sufficient to bias subjects' choices during an auditory discrimination task, but do not establish whether corticostriatal activity contributes to the formation of decisions under normal conditions, in the absence of ChR2 activation. If corticostriatal spikes are important under normal conditions, then suppressing these spikes during the task should lead to an "anti-bias," i.e. a bias in the direction opposite that induced by ChR2 activation. To test this hypothesis, we targeted the expression of the light-activated proton pump Archaerhodopsin-3[3] to corticostriatal neurones using the HSV1-based approach described above (Fig. 3a). Rather than attempting to inactivate all corticostriatal cells—a technically difficult feat whose interpretation might be obscured by the compensatory plasticity common to lesion studies—we sought instead to silence corticostriatal neurones within a restricted region of the tonotopic map.

Pulses of green light in Arch-expressing animals inhibited spiking of putative corticostriatal neurones (Fig. 3b). As predicted, inactivation of corticostriatal neurones biased subjects' choices away from the reward port associated with the frequency band of the inactivation site (Fig. 3c) but did not affect subjects' sensitivity quantified as the slope of the psychometric curve (Fig. S4d). A similar trend was reflected in the subjects' chronometric functions but did not reach significance (Fig. S11kl). Pulses of green light did not affect the behaviour of uninjected control animals (Fig. S5c). These results indicate that corticostriatal neurones in the auditory cortex transmit signals used by rats to make decisions driven by sounds.

These experiments provided us with an opportunity to quantify the contribution of the output of single corticostriatal cells to behaviour. Earlier studies showed that subjects can be trained to detect the artificial stimulation of as few as 6–197 neurones[24] or even a single neurone[25]. Our experiments allow us to estimate the contribution of single neurones to behaviour during normal perception.

We used Arch-GFP fluorescence to estimate the number of neurones silenced in each experiment (Fig. 4b). Using *in vivo* recordings of putative corticostriatal cells, we estimated that the efficiency of inactivation decayed with a space constant of ~564 μm (Fig. 4a, S11). We quantified the number of Arch-expressing neurones within a radius of 1 mm, or approximately two space constants, from the inactivation fiber for each session. The magnitude of choice biases depended on the number of corticostriatal neurones expressing Arch near the fiber (Fig. 4c). Robust choice biases were observed for sites with 1040–2444 Arch-expressing neurones within 1 mm of the fiber, comprising 0.35–0.83% of neurones in that volume. Our observation that inactivation of this minute fraction of cells targeted to corticostriatal neurones could affect behaviour suggests a privileged role of these cells in auditory discrimination.

The size of the neuronal pool accounting for behavioural performance in psychophysical tasks is much smaller than the number neurones which carry signals relevant to the task[26].

The redundancy arising from correlated neuronal firing may restrict the effective size of the pool[26], limiting psychophysical performance. Our results suggest that the finite bandwidth provided by a small number of projection neurones that drive decisions constitutes an additional constraint limiting the effective pool size and therefore psychophysical performance.

We have shown that the striatal projection of the auditory cortex conveys signals that drive behavioural choices during performance of an auditory discrimination task. While our results do not exclude the participation of other parallel pathways, the ubiquity of corticostriatal projections in cortex may provide a general mechanism for control of motor decisions by sensory context[27].

Methods

Viral production

The AAV CAGGS ChR2-Venus plasmid used for non-specific cortical stimulation was a provided by K. Svoboda (HHMI Janelia Farm). AAV CAGGS FLEX ChR2-tdTomato virus used for targeted stimulation of corticostriatal neurons was a gift of A. Kepecs (Cold Spring Harbor Laboratory). AAV FLEX Arch-GFP construct was generated subcloning Arch-GFP from an AAV CAG Arch-GFP plasmid (provided by E. Boyden, MIT) into AAV FLEX backbone from AAV FLEX ChR2-YFP (provided by K. Deisseroth, Stanford University). The plasmid DNA was prepared using standard maxiprep protocols (Qiagen). AAV serotype 2/9 was packaged by the University of North Carolina viral core at the titer of 1–2 $\times 10^{12}$ particles per ml. HSV-mCherry-IRES-iCre (for targeting Arch expression) and HSV-iCre-2A-Venus (for targeting ChR2 expression) constructs were provided by Andreas Luthi (Friedrich Miescher Institute, Switzerland) and packaged by BioVex (Biovex Group Inc.) at the titer of 2.4 $\times 10^{10}$ and 3 $\times 10^{9}$ transducing units per ml.

Animal subjects

Animal procedures were approved by the Cold Spring Harbor Laboratory Animal Care and Use Committee and carried out in accordance with National Institutes of Health standards. Male Long Evans rats (Taconic Farms) were housed with free access to food, but were water restricted following the start of behavioural training. Water was available during task performance (24 μl for each correct trial) and freely available for 15–30 min after the end of each behavioural sessions and for at least 1 hour on days when behavioural sessions were not conducted.

Viral injection

Three to five week old rats were anaesthetised with mixture of ketamine (60 mg/kg of body weight) and medetomidine (0.24 mg/kg) and placed in a stereotaxic apparatus. To target the auditory cortex, part of the temporalis muscle was resected to expose the temporoparietal suture, which was used as a landmark to target injections. For optogenetic experiments, 4 injections were made unilaterally spanning primary auditory cortex at 0.5, 1.5, 2.5 and 3.5 mm from the rostral edge of parietal bone and 1.2 mm from its ventral edge. A small craniotomy was made for each injection and a glass micropipette was inserted perpendicular

to the surface of the brain. Two injections were made at the depths of 400 and 800 μm expelling ~250 nl of virus at each depth. To target the auditory striatum, two small craniotomies were made 2.0 and 2.5 mm caudal of Bregma and 4.5 mm lateral of the midline. Injections were made at depths between 3.5 and 6 mm, 0.5 mm between injection sites, ~100 nl per site. Injections were performed by delivering brief pulses of pressure using Picospritzer II (Parker), each pulse delivering ~2 nl at 0.2 Hz. Rats were monitored during their recovery from surgery and returned to group housing.

Behavioral training

The cloud of tones stimulus consisted of stream of 30 ms overlapping pure tones presented at 100 Hz (i.e. with 10 ms between tone onsets). Eighteen possible tone frequencies were logarithmically spaced between 5 and 40 kHz, a range where rats' hearing thresholds are low and relatively constant[28]. For each trial either the low (5–10 kHz) or the high (20–40 kHz) octave was selected as the target octave. Stimulus strength r determined the difference in the rate of high and low octave tones in the stimulus. Tones were drawn from the target octave with a probability of $(1 + 2r/100)/3$. The stream of tones continued until the rat withdrew from the center port.

Upon reaching the weight of 200–250 g rats were placed on a water deprivation schedule and commenced behavioural training. The rats were placed in a soundproof behavioural chamber and presented with 3 choice ports. The rats were trained to first poke into the center port, wait for the onset the auditory stimulus and select one of the other two ports to receive a water reward (24 μl). Rats were shaped to carry out this sequence using the following procedure. During the first phase of training, water was delivered at the correct choice port as soon as the stimulus was played. The duration of the pre-stimulus delay, during which the rat was required to remain in the center port, was drawn from an exponential distribution whose mean was gradually increased from 0.05 s to 0.3 s. The next phase of training required to the rat to poke at the correct choice port to trigger water delivery, however, the rat was allowed to correct his choice if it made a mistake. Once rats learned to perform the discrimination above chance, they were required to make the correct choice on the first attempt. Error trials were punished with a 4 s timeout (2 s during recording sessions). Initially, rats were trained to discriminate tone cloud stimuli composed of tones entirely either in the high or the low octave ($r = 100$) and were gradually introduced to more and more difficult stimuli.

Sound intensity of individual tones was constant during each trial. To discourage subjects from using loudness differences in discrimination, tone intensity was randomly selected on each trial from a uniform distribution 45–75 dB (SPL) during training. During manipulation and recording sessions, sound intensity was kept constant at 60 dB.

Electrophysiology and optogenetics

Custom-built optical fiber/tetrode arrays were assembled in-house. Each array carried 6 multimodal optical fibers 62.5 μm in diameter with 50 μm core. The fiber tips were sharpened to point using a diamond wheel to improve tissue penetration and increase the angle of the light exit cone. Each fiber was glued to a tetrode and the tetrode tip was cut to

terminate within ~100 μm of the fiber tip. The fiber/tetrode assemblies were mounted on individually movable microdrives. The tetrodes were gold-plated to an impedance of 300 kΩ at 1 kHz and the tetrode/fiber tips were coated with DiI to assist with the identification of fiber tracks in brain tissue.

To implant the fiber/tetrode array, rats were anaesthetised with a mixture of ketamine (40 mg/kg of body weight) and medetomidine (0.16 mg/kg) and placed in a stereotaxic apparatus. A craniotomy was made over the target area (for auditory cortex, 3.5–6.0 mm caudal of Bregma and 6.5–7.0 mm lateral from the midline; for auditory striatum, 2.5–3.5 mm caudal of Bregma and 4–5 mm lateral from the midline). All rats, with the exception of 1 Arch-expressing and 1 uninjected control animal, were implanted in the left hemisphere. The dura was removed and the implant was placed over the target area and fixed in place with dental acrylic. The tetrodes were then lowered until first action potentials were encountered.

To characterize the frequency tuning of stimulation and inactivation sites, the rats were placed in a soundproof chamber and pure tones were played in free field at ~0.5 Hz. Tone frequencies spanned from 1 to 64 kHz and were played in a random order at 30, 50 or 70 dB-SPL. Only sites that significantly responded to sounds ($p < 0.01$, signed-rank test comparing firing rate 5–55 ms following sound onset to 0–50 ms preceding sound onset) were included in the analysis of stimulation and inactivation experiments. To determine the preferred frequency, firing rates in the window 5–55 ms following sound onset were computed for each frequency at 70 dB. The resulting tuning curve was smoothed with a 1/2 octave sliding window. The peak of the smoothed tuning curve was selected as the preferred frequency. Sites tuned to frequencies more than 1 octave outside the range used in the task (below 2.5 kHz) were excluded from analysis.

For optogenetic manipulations, laser light was coupled into a FC/PC parch cord using a FiberPort Collimator (Thor Labs). Laser power was adjusted to produce the desired output at the end of the patch cord. A single implanted fiber was selected for manipulation and coupled to the patch cord. For ChR2 activation, 473 nm laser light (10 mW) was delivered in 1 ms pulses (except at 9 sites corticostriatal stimulation sites, where we used 0.5 ms pulses) at 40 Hz while the rat remained in the center port. For Arch, 530 nm laser light (50 mW) was delivered in 1 ms pulses (except at 6 sites where we used 0.5 ms pulses) at 100 Hz, yielding the average power of 5 mW. To decrease the ability of the rat to detect the stimulation light, a mask LED of a wavelength similar to that of the laser was placed above the center port in the behaviour chamber. The mask LED was activated on control as well as stimulation trials in the same temporal pattern as the laser. Manipulation trials were randomly interleaved among control trials. The optical fiber was advanced at least 300 μm between manipulation sessions.

For action potential recordings, signals were filtered 600–6000 Hz and recorded using the Neuralynx Cheetah 32 system and Cheetah data acquisition software.

Pharmacological inactivation

Two PEEK tubing cannulas (Plastics One) were implanted into the auditory cortex with a separation of ~1 mm. Six stereotrodes were implanted alongside the cannulas spanning 3–4 mm of the auditory cortex to confirm the efficiency of inactivation. One hour before the start of the behavioural session, the animal was briefly anaesthetised with 2% isofluorane and 0.4 μl of drug (during inactivation sessions) or 9 g/l NaCl (during control sessions) was injected at the rate of 0.08 μl/min in both cannulas.

Data analysis: behaviour

Although each trial had a target frequency distribution, which determined which choice port was to be rewarded, since rats sampled the stimulus for a finite period of time, the frequency distribution they experienced might have been substantially different from the target. Therefore, we determined the rate of presentation of high and low tones (f_{high} and f_{low}), i.e. the number of tones divided by the reaction time, that the rats actually heard on each trial. To quantify rats' behaviour, psychometric curves were fit with a logistic regression model:

$$ln\frac{p}{1-p}=\beta_0+\beta_1(f_{high}-f_{low}) \quad (1)$$

where p is the fraction of choices toward the port associated with high frequencies. Parameters β_0 and β_1 measure the bias and slope of the psychometric curve, respectively. To quantify the effects of stimulation or inactivation, we extended the model to incorporate the effects of these manipulations:

$$ln\frac{p}{1-p}=\beta_0+\beta_1(f_{high}-f_{low})+\beta_2 S+\beta_3 S(f_{high}-f_{low})$$

where S is 1 on manipulation trials and 0 on control trials. The choice bias evoked by the manipulation is $\beta_2/(\beta_1+\beta_3)$ tones/s. In experiments where ChR2 or Arch expression was specifically targeted to corticostriatal neurones the interaction term β_3 was not significantly different from 0 and was omitted in estimates of choice bias:

$$ln\frac{p}{1-p}=\beta_0+\beta_1(f_{high}-f_{low})+\beta_2 S$$

The light-evoked choice bias is then β_2/β_1 tones/s. Confidence intervals and p-values for individual manipulation sessions were estimated from standard errors of regression coefficients. To quantify the effects of stimulus strength $|f_{high}-f_{low}|$ on response times t_r, we first used linear regression:

$$t_r=t_0-m\times|f_{\mathrm{high}}-f_{low}|/100$$

Regression slope m estimates $RT_{0tones/s}-RT_{100tones/s}$, the change in response time between ambiguous and easiest trials. To fit subjects' chronometric functions on individual sessions, we calculated the recentered stimulus strength f', such that subjects responded with equal

probability to either choice port at $f' = 0$, using bias β_0 and slope β_1 estimates from the psychometric fit in (1):

$$f' = f_{high} - f_{low} + \beta_0/\beta_1$$

We then fit subjects' response times t_r to the following function[29]:

$$t_r = \frac{k}{f'}\tanh(\beta_1 f') + t_m$$

Parameter t_m can be thought of as the motor component of the response time, and k sets the magnitude of modulation of response times by the stimulus. We found the values of t_m and k that minimized the mean square error of t_r predictions using MATLAB's *fminsearch* function. We measured the shift of the chronometric function produced by stimulation q, adding it to the response time model:

$$t_r = \frac{k}{f' + qS}\tanh(\beta_1(f' + qS)) + t_m$$

To avoid local minima, we reran *fminsearch* 100 times using random starting parameter values and selected the set of parameter estimates with the smallest mean square error. Sites for which the fitting procedure failed to converge or produced extreme estimates of the chronometric shift (>200 tones/s) were excluded from further analysis.

In summary plots, linear regression using ordinary least squares method was used to evaluate the relationship between frequency tuning and stimulation-evoked choice biases. Confidence intervals for regression fits were estimated using bootstrap resampling. A small number of sites (2 of 59 using non-specific cortical stimulation; 4 of 56 using striatal axonal stimulation) produced extreme choice biases (>200 tones/s) outside the stimulus range tested in the task and were excluded from regression analysis. Including these sites did not alter the conclusion that striatal axonal stimulation tended to bias subjects in the direction associated with the preferred frequency of the stimilation site ($p = 0.03$, signed-rank test).

Since we expected that the effects of inactivation would only be detectable when a large fraction of the local population of corticostriatal neurons were silenced, we excluded sites with low Arch expression near the inactivation site (<1000 cells) in the analysis of behavioral effects of Arch-inactivation in Figure 3c. For 2 fibers in one of the rats we could not locate the tracks in histological sections and precisely estimate cell counts. Excluding the behavioral effects of inactivation at these fibers from Figure 3c did not affect our conclusions ($p = 0.014$ for linear regression of choice bias and frequency tuning). Furthermore, the relationship between inactivation choice bias and tuning was unchanged whether we selected sites with >250 neurons ($p = 0.012$) or >500 neurons ($p = 0.0052$) near the fiber.

Data analysis: electrophysiology

To isolate single units, spikes were manually clustered using MClust (MClust-3.5, A.D. Redish et al.). Neurometric functions were computed using the first 200 ms of the auditory response and only included trials where the rat remained in the center port for at least that period of time. We selected neurones whose firing rate during that epoch was ≥ 0.5 Hz. We used leave-one-out cross-validation to determine neurometric thresholds and frequency preference for each neurone. Specifically, for each trial we used ROC-analysis including firing rates on all other trials in the recording session to select a firing rate threshold that best discriminated the frequency content of the auditory stimulus and determine whether the neurone prefers high or low frequency stimuli. Trials where the firing rate was greater than or equal to the discrimination threshold were scored as reporting the preferred frequency of the neurone. The neuronal choices were then fit with a logistic regression model (see eq. 1).

To calculate peristimulus time histograms (PSTHs) neuronal firing rates were smoothed with a causal half-Gaussian kernel (σ = 5 ms). Confidence intervals were derived through bootstrap resampling.

For each Arch-expressing corticostriatal neurone we encountered, we delivered light at different fibers along the array to estimate the maximum distance at which light delivery could reduce the neurone's firing by 50%. We took this distance to be the mean of the distances to the furthest fiber where inactivation was >50% and the closest fiber where inactivation was <50%. The likelihood of inactivation at a given distance was estimated as the fraction of neurones inactivated at that point.

Histology and cell count analysis

At the end of the experiment, rats were deeply anaesthetised with ketamine/medetomedine. Small electrolytic lesions were made by passing 30 μA direct cathodal current through each tetrode for ~10 s, marking the final position of the tetrode tip. The rats were then perfused with 4% paraformaldehyde (PFA), their brains were extracted and postfixed in 4% PFA overnight. The brains were cut into 100 μm sections and mounted using Vectashield (Vector Laboratories) for confocal microscopy. To ensure that HSV-mediated labeling was confined to corticostriatal neurons, we verified that viral expression was absent in adjacent brain structures.

To quantify the depth distribution of opsin expression, we measured the distance of from each fluorescent cell soma to the pia as a fraction of total cortical thickness. To estimate the number of neurones affected by optogenetic manipulations, confocal stacks 50 μm in depth were acquired from alternate sections. The sections were registered using rigid registration maximizing the cross-correlation of fluorescence images of adjacent sections. The locations of ChR2 or Arch expressing neurones were identified manually. Fiber tracks were identified with the help of electrolytic lesions and DiI labeling. Using the locations of the ends of the tracks, we estimated that processing resulted in ~10% shrinkage of the tissue. We estimated the location of the fiber tip during each inactivation session and counted the number of expressing neurones within 1 mm from the fiber at 35 sites illuminated with 5 mW light; at 6 sites illuminated at 2.5 mW we reduced the radius according to square root of the power to

0.7 mm; excluding these sites from the analysis did not affect our conclusions ($p = 0.036$, linear regression of cell count and choice bias). Since we only identified cells within a 50 μm stack every 200 μm, our estimate of the total number of manipulated cells is 4× this count.

Supplementary Material

Refer to Web version on PubMed Central for supplementary material.

Acknowledgments

We thank B. Burbach for technical assistance, members of the Kepecs lab (CSHL) for for the tetrode/fiber drive design, K. Deisseroth (Stanford University), E. Boyden (MIT), K. Svoboda (HHMI, Janelia Farm) and A. Luthi (Friedrich Miescher Institute, Switzerland) for reagents. This work was supported by grants from the Schwartz Foundation and the NIH (grant no. 25041001 & 55120101).

References

1. Nagel G, et al. Channelrhodopsin-2, a directly light-gated cation-selective membrane channel. P Natl Acad Sci USA. 2003; 100:13940–5.
2. Boyden ES, Zhang F, Bamberg E, Nagel G, Deisseroth K. Millisecond-timescale, genetically targeted optical control of neural activity. Nat Neurosci. 2005; 8:1263–8. [PubMed: 16116447]
3. Chow BY, et al. High-performance genetically targetable optical neural silencing by light-driven proton pumps. Nature. 2010; 463:98–102. [PubMed: 20054397]
4. Ding L, Gold JI. Caudate encodes multiple computations for perceptual decisions. J Neurosci. 2010; 30:15747–59. [PubMed: 21106814]
5. Kimchi EY, Laubach M. Dynamic encoding of action selection by the medial striatum. J Neurosci. 2009; 29:3148–59. [PubMed: 19279252]
6. Reynolds JN, Hyland BI, Wickens JR. A cellular mechanism of reward-related learning. Nature. 2001; 413:67–70. [PubMed: 11544526]
7. Pasupathy A, Miller EK. Different time courses of learning-related activity in the prefrontal cortex and striatum. Nature. 2005; 433:873–6. [PubMed: 15729344]
8. Beckstead RM, Domesick VB, Nauta WJ. Efferent connections of the substantia nigra and ventral tegmental area in the rat. Brain Res. 1979; 175:191–217. [PubMed: 314832]
9. Hopkins DA, Niessen LW. Substantia nigra projections to the reticular formation, superior colliculus and central gray in the rat, cat and monkey. Neurosci Lett. 1976; 2:253–259. [PubMed: 19604767]
10. Felsen G, Mainen ZF. Neural substrates of sensory-guided locomotor decisions in the rat superior colliculus. Neuron. 2008; 60:137–48. [PubMed: 18940594]
11. Kreitzer AC, Malenka RC. Striatal plasticity and basal ganglia circuit function. Neuron. 2008; 60:543–54. [PubMed: 19038213]
12. Allen Brain Institute. Allen Mouse Connectivity Atlas. 2012. URL connectivity.brain-map.org
13. McGeorge AJ, Faull RL. The organization of the projection from the cerebral cortex to the striatum in the rat. Neuroscience. 1989; 29:503–37. [PubMed: 2472578]
14. Bordi F, LeDoux J. Sensory tuning beyond the sensory system: an initial analysis of auditory response properties of neurons in the lateral amygdaloid nucleus and overlying areas of the striatum. J Neurosci. 1992; 12:2493–2503. [PubMed: 1613543]
15. Bordi F, LeDoux J, Clugnet MC, Pavlides C. Single-unit activity in the lateral nucleus of the amygdala and overlying areas of the striatum in freely behaving rats: rates, discharge patterns, and responses to acoustic stimuli. Behav Neurosci. 1993; 107:757–69. [PubMed: 8280386]
16. Salzman CD, Britten KH, Newsome WT. Cortical microstimulation influences perceptual judgements of motion direction. Nature. 1990; 346:174–7. [PubMed: 2366872]

17. Sally SL, Kelly JB. Organization of auditory cortex in the albino rat: sound frequency. J Neurophysiol. 1988; 59:1627–1638. [PubMed: 3385476]
18. Uchida N, Mainen ZF. Speed and accuracy of olfactory discrimination in the rat. Nat Neurosci. 2003; 6:1224–9. [PubMed: 14566341]
19. Lilley CE, et al. Multiple immediate-early gene-deficient herpes simplex virus vectors allowing efficient gene delivery to neurons in culture and widespread gene delivery to the central nervous system in vivo. J Virol. 2001; 75:4343–56. [PubMed: 11287583]
20. Lima SQ, Hromádka T, Znamenskiy P, Zador AM. PINP: a new method of tagging neuronal populations for identification during in vivo electrophysiological recording. PloS One. 2009; 4:e6099. [PubMed: 19584920]
21. Ciocchi S, et al. Encoding of conditioned fear in central amygdala inhibitory circuits. Nature. 2010; 468:277–82. [PubMed: 21068837]
22. Reiner A, Jiao Y, Del Mar N, Laverghetta AV, Lei WL. Differential morphology of pyramidal tract-type and intratelencephalically projecting-type corticostriatal neurons and their intrastriatal terminals in rats. J Comp Neurol. 2003; 457:420–40. [PubMed: 12561080]
23. Reale RA, Imig TJ. Auditory cortical field projections to the basal ganglia of the cat. Neuroscience. 1983; 8:67–86. [PubMed: 6835523]
24. Huber D, et al. Sparse optical microstimulation in barrel cortex drives learned behaviour in freely moving mice. Nature. 2008; 451:61–4. [PubMed: 18094685]
25. Houweling AR, Brecht M. Behavioural report of single neuron stimulation in somatosensory cortex. Nature. 2008; 451:65–8. [PubMed: 18094684]
26. Britten KH, Shadlen MN, Newsome WT, Movshon JA. The analysis of visual motion: a comparison of neuronal and psychophysical performance. J Neurosci. 1992; 12:4745–65. [PubMed: 1464765]
27. Jiang H, Stein BE, McHaffie JG. Physiological evidence for a trans-basal ganglia pathway linking extrastriate visual cortex and the superior colliculus. J Physiol. 2011; 589:5785–99. [PubMed: 21986209]
28. Kelly JB, Masterton B. Auditory sensitivity of the albino rat. J Comp Physiol Psych. 1977; 91:930–6.
29. Palmer J, Huk A, Shadlen M. The effect of stimulus strength on the speed and accuracy of a perceptual decision. J Vis. 2005; 5:376–404. [PubMed: 16097871]

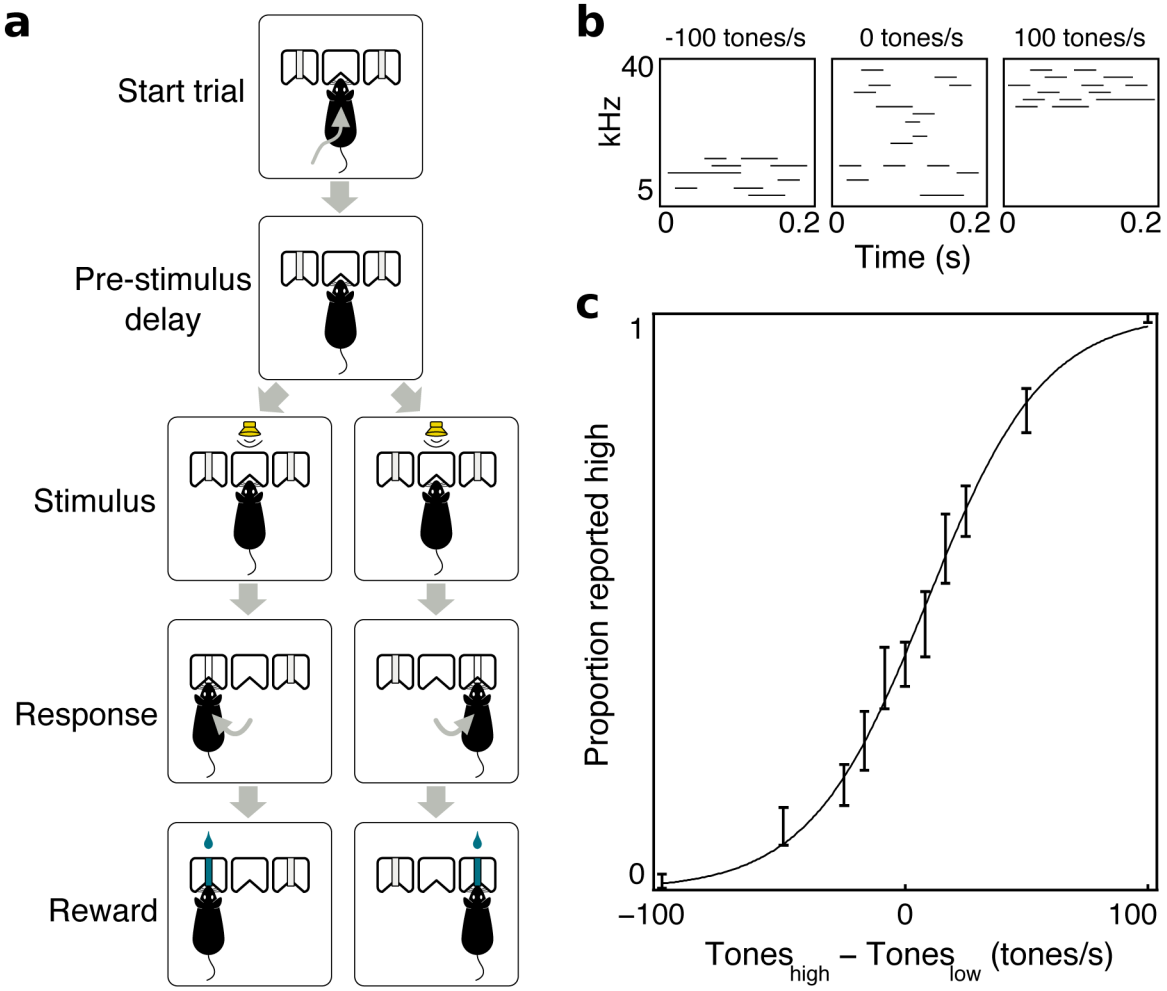

Figure 1. Cloud of tones task

a, Layout of the behavioural task.

b, Example stimulus spectrograms at −100, 0 and +100 tones/s.

c, Psychometric curve from a single rat (error bars - 95% confidence interval).

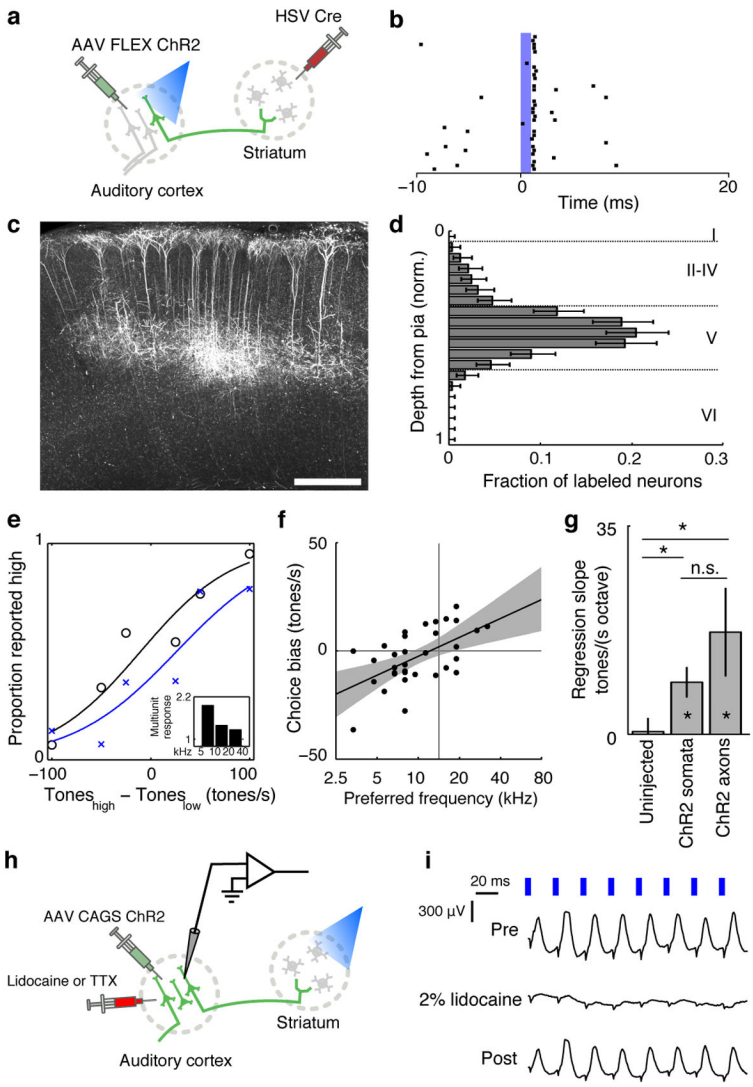

Figure 2. ChR2 stimulation of corticostriatal neurones biases subjects' choices

a, Strategy targeting ChR2 expression to corticostriatal neurones.

b, A presumed corticostriatal neurone with a short latency light-evoked response (~1 ms). Blue bar indicates the timing of the light pulse (10 mW, 1 ms duration).

c, Depth distribution of ChR2 expression. Dashed lines mark the approximate location of layer boundaries. Error bars - 95% confidence intervals.

d, ChR2 expression in corticostriatal neurones. Scale bar - 500 μm.

e, Psychometric performance during a behavioural session on control (black) trials and during stimulation of corticostriatal neurones (blue). $p = 0.02$ for stimulation-evoked choice bias. Inset shows frequency tuning of multiunit responses normalized to baseline, binned by octave.

f, Across the population, direction and magnitude of choice biases evoked by stimulation depends on the frequency preference of the stimulation site. $n = 33$ sites from 2 rats, $p = 0.0006$ for linear regression of choice bias and frequency preference. Gray shading is 95% confidence interval for regression line.

g, Dependence of choice bias on preferred frequency of the stimulation site in uninjected controls, and during specific stimulation of corticostriatal neurons and their axons. * - $p < 0.05$, n.s. - not significant, error bars are standard error through bootstrap.
h, Strategy for inactivation of recurrent cortical activity during stimulation of striatal axons.
i, Lidocaine infusion into the auditory cortex reversibly abolishes antidromic light-evoked LFP responses.

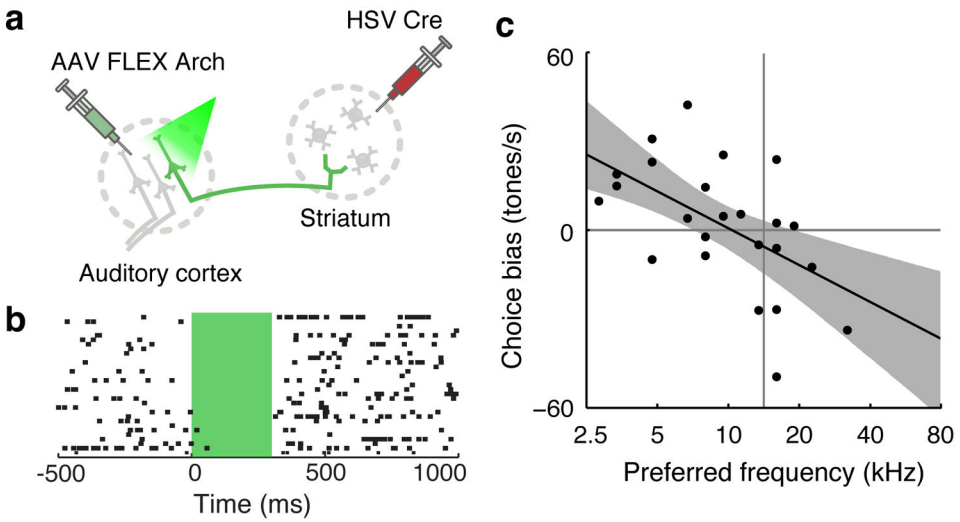

Figure 3. Arch-mediated inactivation of corticostriatal neurones anti-biases subjects' choices

a, Strategy targeting Arch expression to corticostriatal neurones.

b, Activity of a presumed corticostriatal neurone inhibited by pulses of green light. Green shading shows the timing of the light pulse (300 ms, 5 mW).

c, Inactivation biased choices away from the direction associated with the preferred frequency of the inactivation site. $n = 24$ sites from 3 rats, $p = 0.0043$ for linear regression of choice bias and frequency preference.

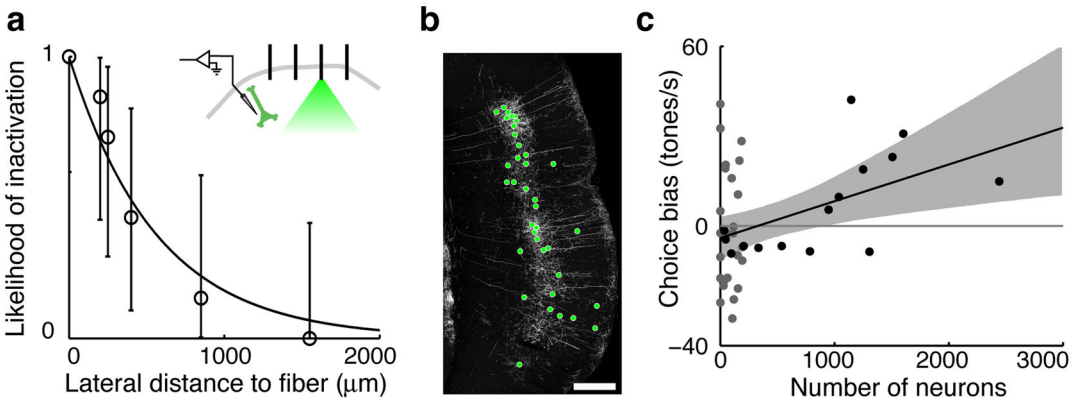

Figure 4. Estimation of numbers of neurons affected by Arch-inactivation

a, The likelihood of silencing for Arch-expressing corticostriatal neurones as a function of distance from the fiber (n = 7). Error bars are 95% binomial confidence intervals.

b, Somata of neurones expressing Arch-GFP (green circles) identified in a fluorescence image of the auditory cortex at the end of an inactivation experiment. Scale bar - 500 μm.

c, Effects of inactivation at sites tuned <10 kHz or >20 kHz were correlated with the number of Arch-expressing neurones near the fiber. n = 41 sites from 5 rats, p = 0.021 for linear regression of choice bias and neuron number. Data for 2 of 5 rats, for which Arch expression was low throughout the auditory cortex (on average 72±69 cells per site), are in gray.